Chem. Senses 36: 771–780, 2011

doi:10.1093/chemse/bjr052
Advance Access publication June 15, 2011

Expression and Distribution of Facilitative Glucose (GLUTs) and Monocarboxylate/H^+ (MCTs) Transporters in Rat Olfactory Epithelia

Alexia Nunez-Parra[1,3,*], Christian Cortes-Campos[2,*], Juan Bacigalupo[3,4], Maria de los Angeles Garcia[2], Francisco Nualart[2] and Juan G. Reyes[1]

[1]Instituto de Química, Facultad de Ciencias, Pontificia Universidad Católica de Valparaíso, Av. Brasil 2950, Valparaíso 2340025, Chile, [2]Departamento de Biología, Facultad de Ciencias, Universidad de Chile, Las Palmeras 3425, Ñuñoa, Santiago 7800024, Chile, [3]Institute for Cell Dynamics and Biotechnology, Universidad de Chile, Plaza Ercilla 847, Santiago 8370450, Chile and [4]Departamento de Biología Celular, Facultad de Ciencias, Universidad de Concepción, Barrio Universitario, Concepción 4070043, Chile

Correspondence to be sent to: Alexia Nunez-Parra, Bioscience Research Bldg R-1239, University of Maryland, College Park, MD 20742, USA. e-mail: anunez1@umd.edu

*These authors contributed equally to this work.

Accepted May 18, 2011

Abstract

Cell-to-cell metabolic interactions are crucial for the functioning of the nervous system and depend on the differential expression of glucose transporters (GLUTs) and monocarboxylate transporters (MCTs). The olfactory receptor neurons (ORNs) and supporting cells (SCs) of the olfactory epithelium exhibit a marked polarization and a tight morphological interrelationship, suggesting an active metabolic interaction. We examined the expression and localization of MCTs and GLUTs in the olfactory mucosa and found a stereotyped pattern of expression. ORNs exhibited GLUT1 labeling in soma, dendrites, and axon. SCs displayed GLUT1 labeling throughout their cell length, whereas MCT1 and GLUT3 localize to their apical portion, possibly including the microvilli. Additionally, GLUT1 and MCT1 were detected in endothelial cells and GLUT1, GLUT3, and MCT2 in the cells of the Bowman's gland. Our observations suggest an energetic coupling between SCs and Bowman's gland cells, where glucose crossing the blood–mucosa barrier through GLUT1 is incorporated by these epithelial cells. Once in the SCs, glucose can be metabolized to lactate, which could be transported by MCTs into the Bowman's gland duct, where it can be used as metabolic fuel. Furthermore, SCs may export glucose and lactate to the mucous layer, where they may serve as possible energy supply to the cilia.

Key words: chemosensory cilia, metabolic coupling, olfactory receptor neuron, supporting cell

Introduction

The olfactory mucosa (OM) consists of 2 layers, the olfactory epithelium (OE) and the lamina propria. In rodents, the OE is formed by olfactory receptor neurons (ORNs), supporting cells (SCs), basal cells, and Bowman's gland duct cells. The bipolar ORNs span the epithelium, projecting a single dendrite to the mucosal surface and a thin unmyelinated axon to the olfactory bulb. ORN nuclei are aligned two-thirds from the base of the epithelium and their dendrites terminate in a structure called the knob, from where the chemosensory cilia responsible for odor transduction emanate. The SCs have a columnar shape and also span the epithelium, bearing microvilli in their apical surface. In the apical portion of the epithelium, the SCs wrap the dendrites of the ORNs, a microanatomy consistent with a functional relationship between these 2 cell types. The ducts of the Bowman's glands originate in the lamina propria and project to the epithelial mucosal surface (Farbman 1992; Nomura et al. 2004). The capillaries of the OM run along the lamina propria, far from the somata of the sensory neurons. Interestingly, the endothelial cells of the capillaries express glucose transporter 1 (GLUT1) and the tight junction proteins, suggesting the presence of a blood–mucosa barrier (Hussar et al. 2002). The OE cytoarchitecture resembles that of other neural networks, comprising neurons, glial cells, and endothelium, suggesting the existence of cell–cell metabolic interactions.

A general feature of the nervous system is that neurons are surrounded by cells that act as intermediaries in the exchange of metabolites with the blood. Accordingly, some of these cells (neurons, glia, and endothelial cells) differentially express metabolite transporters isoforms, like GLUTs and monocarboxylate transporters (MCTs, e.g., Pellerin et al. 2007; Cortes-Campos et al. 2011). In general, several isoforms of the glucose facilitative transporters have been identified in the brain (GLUT1, 2, 3, 4, 5, 6, 8, and 10; for review, see Simpson et al. 2007). These studies demonstrated that GLUT1 and GLUT3 are the most widely expressed transporters in the central nervous system (CNS). Endothelial cells express GLUT1, which transports glucose from the blood to the interstitial space, being essential for glucose transport through the blood–brain barrier (Takata et al. 1997; Nualart et al. 1999; Garcia et al. 2001). Astrocytes also express GLUT1, allowing the utilization of glucose in their metabolism (Yu and Ding 1998). Interestingly, it has been shown that glutamate (the main excitatory neurotransmitter in the brain) can also be transported through a Na^+-driven mechanism into astrocytes. The resulting increase in intracellular Na^+ concentration further activates an Na^+/K^+ ATPase, promoting astrocytic glycolysis and lactate production (Pellerin and Magistretti 1994). Astrocytes also express MCT1 and MCT4, by which these cells can release lactate to the extracellular space (Pellerin et al. 2005). On the other hand, neurons express MCT2 (Pierre et al. 2002), the highest affinity MCT, allowing uptake of lactate from the extracellular space which they use as respiratory fuel. Additionally, neurons in the CNS express GLUT3, a high-affinity glucose transporter, and incorporate to a lesser extent glucose from the intercellular space (Gerhart et al. 1989; Castro et al. 2007). This scenario is not exclusive to astrocytes and neurons as the metabolic cell-to-cell interaction has been also shown between hypothalamic tanycytes and neurons (Millan et al. 2010; Cortes-Campos et al. 2011) and in a peripheral sensory organ like the retina, between Müller and photoreceptors cells (Wood et al. 2005).

In this work, we determined in the rat OE the expression of GLUT1, 2, 3, and 5. Using immunohistochemistry, we also examined the distribution of GLUT1 and 3, as representatives of medium- and high-affinity glucose facilitative transporters, respectively (e.g., Zhao and Keating 2007). Furthermore, we studied the expression of MCT1, 2, and 4 and the distribution of MCT1 and 2 in this tissue, as representatives of medium- and high-affinity MCTs (e.g., Morris and Felmlee 2008). Our results show that OE cells differentially express GLUT1, GLUT3, MCT1, and MCT2, suggesting an integrated substrate handling and metabolism between SCs, cells of the Bowman's gland and duct, and potentially ORNs.

Materials and methods

Animals

Adult male Sprague–Dawley rats were used throughout the experiments. Animals were kept in a 12 h light:dark cycle with food and water ad libitum. The handling and discarding of the animals were performed in agreement with the biosecurity regulations (*Biosecurity Manual of the Chilean National Committee for Science and Technology*, CONICYT, 2008) and the procedures indicated in the publication *Guide for Care and Use of Laboratory Animals* (National Academy of Science, 1996).

Reverse transcription–polymerase chain reaction

The total RNA of rat OM, muscle, choroid plexus (CP), liver, small intestine (SI), and Neuro2A cell line was isolated using Trizol (Invitrogen). For reverse transcriptase–polymerase chain reaction (RT–PCR), 3–4 μg of RNA was incubated in 20 μL reaction volume containing 5× buffer for M-MulV RT, 20 U RNAse inhibitor, 1 mM dNTPs, 2.5 μM oligo(dt)18 primer, and 10 U revertAidTM H minus M-MuLV reverse transcriptase (Fermentas International Inc.) for 5 min at 37 °C, followed by 60 min at 42 °C and 10 min at 70 °C. Parallel reactions were performed in the absence of reverse transcriptase to control for contaminant DNA. For amplification, a cDNA aliquot (1 μL) in a volume of 12.5 μL containing 10× buffer PCR without $MgCl_2$ (Fermentas International Inc.), 10 μM dNTPs, 25 μM $MgCl_2$, 0.3125 U of *Taq* DNA polymerase (Fermentas International Inc.), and 10 μM of each primer were incubated at 95 °C for 5 min, 35 cycles (5 s at 95 °C, 30 s at 55 °C, and 40 s at 72 °C), and 7 min at 72 °C. PCR products were separated by 1.2% agarose gel electrophoresis and visualized by staining with ethidium bromide. The following set of primers was used to analyze the expression of MCT1: sense 5′-GGG AAG GTG GAA AAA CTC AA-3′, antisense 5′-ACA CTC CAT TCG CAA CAA CA-3′ (expected product of 400 bp); MCT2: sense 5′-CAG GAG GTC CCA TCA GTA GT-3′, antisense 5′-ACT TTT AGA CTT CGC AGC AC-3′ (expected product of 416 bp); MCT4: sense 5′-TGC GGC CCT ACT CTG TCT AC-3′, antisense 5′-TCT TCC GAT GCA GAA GAA G-3′ (expected product of 369 bp); GLUT1: sense 5′-CAT GTA TGT GGG GAG GTG T-3′, antisense 5′-GAC GAA CAG CGA CAC CAC AG-3′ (expected product of 559 bp); GLUT2: sense 5′-GGC TAA TTT CAG GAC TGC TT-3′, antisense 5′-TTT CTT TGC CCT GAC TTC CT-3′ (expected product of 278 bp); GLUT3: sense 5′-GGG CAT GAT TGG CTC TTT TT-3′, antisense 5′-GGG CTG CGC TCT GTA GGA TA-3′ (expected product of 386 bp); GLUT5: sense 5′-TTG GCC TTC GAG TCT CTT-3′, antisense 5′-GTC CCC AAA GCT CTA CCA CA-3′ (expected product of 483 bp). Additionally, the following set of primers was used to analyze the expression of β-actin: 5′-GCT GCT CGT CGA CAA CGG CTC-3′ and antisense: 5′ CAA ACA TGA TCT GGG TCA TCT TCT C-3′ (expected product of 353 bp).

Immunofluorescence

Rat OM was dissected and fixed directly by immersion in Bouin's solution (750 mL of saturated picric acid, 250 mL

of 37% formaldehyde, and 50 mL of glacial acetic acid). For immunostaining, samples were dehydrated in graded alcohol solutions and embedded in paraffin. Sections (7 μm) were obtained and mounted on poly-L-lysine–coated glass slides. For immunohistochemical analyses, we used the following antibodies and dilutions: chicken anti-MCT1 (1:50, Millipore, Cat# AB1286, antigen: LQNSSGDPAEEESPV), chicken anti-MCT2 (1:100, Millipore, Cat# AB1287, antigen: NTHNPPSDRDKESSI), rabbit anti-GLUT1 (1:1000, East Acres, antigen: last C-terminal 13-aa peptide from Human Glut-1), rabbit anti-GLUT3 (1:50, Alpha Diagnostic International, Inc., Cat# GT31-A, antigen: last C-terminal 12-aa peptide from Mouse), goat anti-olfactory marker protein (OMP) (1:2000, Wako Chemical, Inc., Cat# 544-10001-WAKO), and mouse anti-cytokeratin 18 (1:100, Sigma-Aldrich, Cat# C8541). Sections were incubated with the antibodies overnight at room temperature in a humid chamber. The antibodies were diluted in a Tris–HCl buffer (pH 7.8) containing (in mM) 8.4 NaH_2PO_4, 3.5 KH_2PO_4, 120 NaCl, and 1% bovine serum albumin. After extensive washing, the sections were incubated with the primary antibodies overnight and subsequently with Cy2-, Cy3-, or Cy5-labeled secondary antibodies (1:200, Jackson Immuno Research). The slides were analyzed using single plane confocal images (D-Eclipse C1 Nikon).

Immunoblotting

Total protein extracts were obtained from rat cerebral cortex or OM by homogenizing the tissue in buffer A (0.3 mM sucrose, 3 mM dithiothreitol, 1 mM ethylenediaminetetraacetic acid, 100 μg/mL phenylmethylsulfonyl fluoride, 2 μg/mL pepstatin A, 2 μg/mL leucopeptin, and 2 μg/mL aprotinin) and sonicated 3–5 times for 10 s at 4 °C. Proteins were resolved by sodium dodecyl sulfate–polyacrylamide gel electrophoresis (50 or 180 μg/lane) in a 5–15% (w/v) polyacrylamide gel, transferred to polyvinylidene difluoride (PVDF) membranes (0.45 μm pore, Amersham Pharmacia Biotech), and probed for 2 h at 4 °C with, rabbit anti-GLUT3 (1:4000), rabbit anti-GLUT1 (1:10000), chicken anti-MCT1 (1:4000), or chicken anti-MCT2 (1:000). After extensive washing, the PVDF membranes were incubated with peroxidase-labeled anti-rabbit or peroxidase-labeled anti-chicken IgY (1:1000; Jackson Immuno Research) for 1 h at 4 °C. The reaction was developed using the enhanced chemoluminescence western blotting analysis system (Amersham Biosciences). Negative controls consisted of incubating the membrane with a preabsorbed antibody (anti-MCT1 1:100, anti-GLUT3 1:100, anti-MCT1 1:1000, or MCT4 1:500 with 100 μg/mL inductor peptide incubated at 4 °C overnight).

Image analysis

To corroborate the colocalization of different antigens, we measured the Pearson's coefficient (Rr) in regions of interest (ROIs) of the images, using the Image Pro-Plus software. This coefficient measures the overlapping level between the pixels of 2 fluorescent channels, going from –1 to +1 (100% of colocalization, Manders et al. 1992). The Rr measured for OMP and CYT18 immunolabeling were 0.34 and 0.39 for ORN and SC soma, respectively (Table 1), most likely reflecting a tight relationship between the 2 kinds of cells and the subsequent optical cross between fluorescent signals but not colocalization. Thus, for our colocalization analysis, we defined Pearson coefficient intensities of colocalization in 2 levels: $0 \leq Rr \leq 0.4$, no colocalization; $0.41 \leq Rr \leq 1$, colocalization.

Results

Messenger RNA expression of facilitative GLUTs in the OM

Using the RT–PCR technique, the messenger RNA (mRNAs) of GLUTs 1 and 3 isoforms were found in the OM, whereas GLUT2 and GLUT5 were absent in this tissue (Figure 1A). Every RT–PCR gel included, as positive control, a sample of a tissue or cell line where the presence of the respective transporter had been reported previously, that is, CP for GLUT1 (Kumagai et al. 1994; Vannucci 1994), rat liver (L) for GLUT2 (Lachaal et al. 2000; Eisenberg et al. 2005), the N2A cell line for GLUT3 (Shin et al. 2004), and SI for GLUT5 (Rand et al. 1993).

GLUT1 and 3 immunolocalization

To attain a more precise localization of those GLUTs evidenced by RT–PCR in OM we determined the expression of GLUT1 and 3 in the different OM cell types by immunofluorescence and confocal microscopy. The specificity of the primary antibodies used in our study was tested through western blot analysis, utilizing an OM preparation and total brain extract as positive controls and preabsorbed antibodies as a nonspecific primary antibody–binding control (Figures 1B and 3B). Our results confirmed the OE expression of GLUT1 and 3. Furthermore, in the OE, a low molecular weight GLUT1 (45 kDa) was found, unlike the low and high (55 kDa) molecular weight GLUT1 found in brain (Maher et al. 1994; Garcia et al. 2003). GLUT1 and GLUT3 showed a differential localization in the different cell types that comprise the OE. To identify the different cell types present in the OE, we colabeled the cells with an antibody against OMP, a marker for mature ORNs (Kream and Margolis 1984; Nakashima et al. 1985; Weiler and Benali 2005) and an anti-cytokeratin 18 antibody (CYT18), as supporting and Bowman's gland cell marker (Asan and Drenckhahn 2005). In our samples, these 2 antibodies did not label ORN's cilia and SC's microvilli. All the images shown throughout our study correspond to thin optical slices (0.5–1 μm), which was likely the reason why few ORNs were stained in each sample. Interestingly, a polarized distribution of GLUT1 and GLUT3 was observed in the OM (Figure 2). Our result confirmed the observations of Hussar et al. (2002), showing a high expression of GLUT1 in the endothelial cells of the capillaries of the lamina propria (Figure 2I). However, GLUT1 was also expressed in other structures of the OM

Table 1 Pearson's correlation coefficient (Rr) for double immune-labeling and different ROIs

Immune labeling	ROI	Rr	Conclusion
OMP-CYT18	OE, soma SC	0.34	For Rr ≥ 0.41 a possible colocalization is considered
	OE, soma ORN	0.39	
GLUT1-OMP	ORN, knobs	0.39	—
	ORN, dendrites	0.47	+ On ORN dendrite
	ORN, soma	0.50	+ On ORN soma
	LP, nerve bundle	0.56	++ On nerve bundles
GLUT1-CYT18	OE, outmost region	0.24	—
	SC, apical soma	0.57	++ On SC
	SC, basal projection	0.60	++ On SC
	LP, Bowman's gland	0.57	++ On Bowman's gland
GLUT3-OMP	ORN, cilliary zone	0.11	—
	Cilliary zone + dendrites of ORN	0.04	—
MCT1-OMP	OE apical, ORN dendrites, knobs	0.14	—
MCT1-CYT18	OE, outmost region	0.04	—
	SC, soma	0.57	++ On SC soma
MCT2-OMP	ORN, knobs	0	—
	ORN, soma	0.40	—
	LP, Bowman's gland	0.05	—
	LP, nerve bundle	0.05	—
MCT2-CYT18	SC, soma	0.40	—
	LP, nerve bundle	0.16	—
	LP, Bowman's gland	0.52	++ On Bowman's gland
MCT1-GLUT1	OE, outmost region	0.05	—
	ORN/SC, soma	0.62	++
MCT1-GLUT3	OE, apical	0.60	++

CYT-18, cytokeratine 18; LP, lamina propria.

(Figure 2A,E,I). For instance, GLUT1 was present throughout the OE (Figure 2 A–H), where it colocalized with OMP in the ORN somata and dendrites with no clear overlapping in the knobs (Figure 2C,D, arrowhead and arrow). To corroborate our results, we measured the overlap between the 2 signals and calculated the Pearson's correlation coefficient (Rr) for several ROIs, assigning 2 levels of colocalization to our analysis (see Materials and methods): $0 \leq Rr \leq 0.4$, no colocalization; $0.41 \leq Rr \leq 1$, colocalization. In this case, Rrs of 0.50, 0.47, and 0.39 were obtained for ORN's soma, dendrite, and knob, respectively (Table 1), supporting the idea that GLUT1 is present in the somatic and dendritic regions of ORNs. GLUT1 was also present in the apical region (Rr = 0.57) and extensions of the SCs (Rr = 0.60) (Figure 2E–H, arrow and arrowhead, respectively). In the lamina propria, GLUT1 was present in endothelial cells of the capillaries and in cells of the Bowman's glands (Figure 2I–L, Rr = 0.57).

The morphology and localization of the structures stained with GLUT1 in the OM suggest that this transporter is expressed in the nerve bundles (most likely surrounding the axons) and in ensheathing cells (Figure 2I–L, arrowhead and arrow, respectively).

Interestingly, GLUT3 was mainly and robustly expressed in the apical portion of the OE cells, presumably in the apical somata region and microvilli of the SCs and/or in ORN cilia (Figure 2M–P, arrow). There was no overlapping between GLUT3 and OMP in the dendritic area (Rr = 0.035).

mRNA expression of MCTs in the OM

MCTs isoforms 1 and 2 mRNAs were found in the OM, whereas MCT4 was absent in this tissue (Figure 3A). Every RT–PCR gel included, as positive control, a sample of muscle homogenate, where the presence of the respective

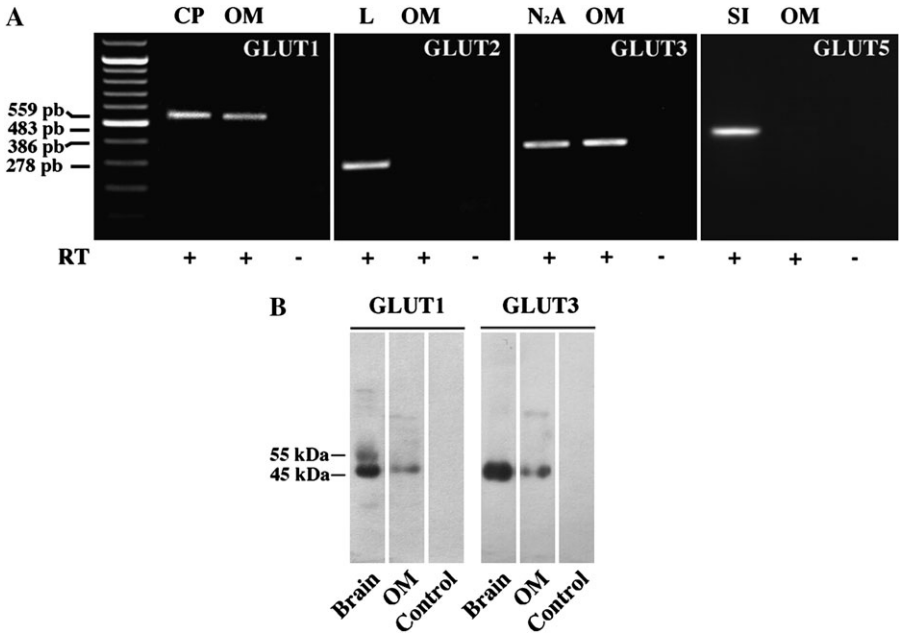

Figure 1 mRNA and protein analysis of GLUT expression in the OM. **(A)** Positive labeling for GLUT1 and GLUT3 mRNA. CP: choroid plexus; L: liver; N_2A: Neuro-2A cell line; SI: small intestine; (-): negative control. **(B)** GLUT1 and GLUT3 are expressed in OM. Total brain extract was used as positive control. Preabsorbed antibodies were used as a nonspecific primary antibody–binding control.

transporters was previously demonstrated (Garcia et al. 1995; Bonen et al. 2006).

MCT1 and MCT2 immunolocalization

Once MCT1 and MCT2 mRNAs were determined in the OM, we studied the localization of MCT1 and MCT2 with immunofluorescence. Through western blot analysis, we confirmed the presence of MCT1 and MCT2 proteins in the OM and controlled for the nonspecific primary antibody binding used in our study (Figure 3B). The 2 transporters displayed a polarized distribution in the OM. MCT1 was abundantly expressed in the epithelium (Figure 4A,B,C,D), where it colocalized with CYT18 (Figure 4A–b3, arrow, Rr = 0.57). Interestingly, no colocalization with CYT18 was evident in the most apical region of the OE (Rr = 0.04, Figure 4b1–b3, arrowhead). In addition, no overlap between OMP and MCT1 signals in the somata or in the ORN knobs was observed (Figure 4d3, Rr = 0.14). As previously reported (Chiry et al. 2006), there was a robust MCT1 expression in the endothelial cells of the capillaries of the lamina propria (Figure 4d3, insert). On the other hand, MCT2 is presumably present in the basal processes of the SCs (Figure 4E–f3, asterisks) and in the ducts of the Bowman's glands (Figure 4E–h3, arrow). In the lamina propria, MCT2 colocalized with CYT18 in the Bowman's gland cells (Figure 4E–f3, arrowhead, Rr = 0.52).

To confirm our results, we performed dual labeling immunofluorescence for MCT1 with GLUT1 and GLUT3 (Figure 5). As expected, MCT1 and GLUT1 signals colocalized in the upper edge of the SC nuclear layer (Figure 5A–b3, arrowhead, Rr = 0.62), whereas MCT1 but not GLUT1 was expressed in the outermost layer (Figure 5A–b3, arrow). In addition, in agreement with our results, MCT1 and GLUT3 had different expression levels in the apical region of the OE (Figure 5C-d3). Below the apical border of the OE, MCT1 (observed only in SCs, not in ORNs; Figure 4) and GLUT3 signals overlapped (Rr = 0.60), suggesting that GLUT3 was expressed in the SCs (Figure 5d1–d3, arrow). No colocalization of MCT1 and GLUT3 was observed in the most apical level of the microvillar and ciliary layer (Figure 5d1–d3, white arrowhead; Rr = 0.05). In addition, GLUT3 was markedly expressed in the cells of the Bowman's gland of the lamina propria, where there was no MCT1 labeling (Figure 5C, asterisk, see also Figure 2M).

Discussion

It was previously demonstrated that GLUT1 was present in the endothelial cells of the capillaries of the OM and also that the different tight junction proteins (i.e., occludin, claudins and zonula occludens) were located in the capillaries and in the apical portion of the OE (Hussar et al. 2002; Steinke et al. 2008; Tang et al. 2009). These results suggest that in order to access the ORN axons and reach the most apical region of the OE cells, such as the chemosensory cilia, the nutrients from the blood must cross the endothelial barrier. Thus, it seems reasonable that endothelial cell-mediated transport and intercellular transport between epithelial cells play a key role on the supply of blood borne substrates to the OE cells. This hypothesis is supported by the close

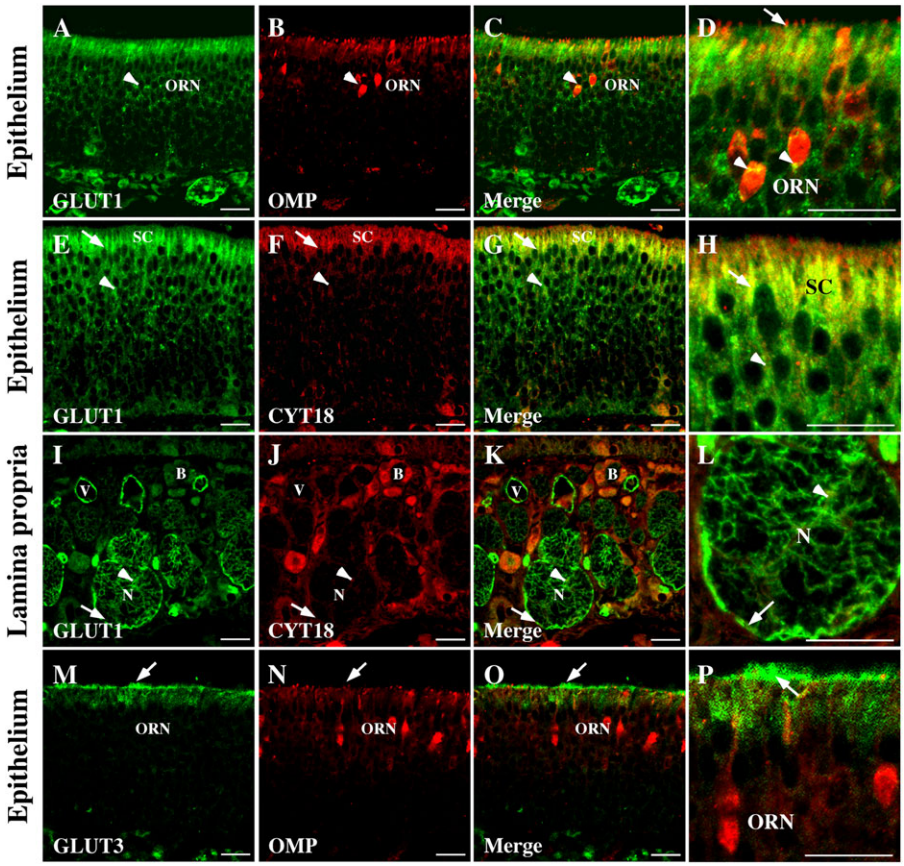

Figure 2 Cellular distribution of GLUT1 **(A–L)** and GLUT3 **(M–P)** in the OM. OMP was used to identify ORN (B) and CYT18 to identify SCs and Bowman's gland cells (F, J). GLUT1 colocalized with OMP in the soma of the ORNs (C and higher magnification view in D, arrowhead) but not in the ORN knobs (D, arrow). GLUT1 and CYT18 expression overlapped in SCs (G–H, arrow). In the lamina propria (I–L), GLUT1 was present in endothelial cells of the blood vessels in the nerve bundles (higher magnification is shown in L, arrowhead), in ensheathing cells (arrow), and in the Bowman's gland where it colocalized with CYT18 (K). GLUT3 (M–P) was located in the microvillar region and the most apical portion of the OE (arrow). Scale bar, 100 μm; B, Bowman's gland; N, nerve bundle; V, blood vessel.

morphological relationship between OE SCs and the dendrites of the olfactory neurons (Nomura et al. 2004).

Our results indicate that in addition to the mucosal endothelial cells (Hussar et al. 2002), GLUT1 is present in the ensheathing cells surrounding ORN axons, the Bowman's gland cells in the lamina propria, and in the OE SCs. Our data suggest that glucose, traveling from the blood stream to the ORNs, overcomes an endothelial barrier in a step mediated by GLUT1 and, once in the lamina propria, is incorporated into the ensheathing cells surrounding the axon bundles by GLUT1. Glucose may also be transported by GLUT1 into SCs, where it was found pronouncedly expressed, but also through the same transporter into ORNs somata or dendrites. The substantial expression of GLUT1 in the apical zone of SCs suggests that glucose from the capillaries may reach the apical surface of such cells, from where it may be transported out to the mucus. On the other hand, the immunofluorescence data seems to indicate that the microvillar layer and apical epithelial zone express GLUT3. With the present data, we cannot rule out the possibility that ORNs cilia might also express GLUT3 or other GLUTs, not considered in this study. However, an extended immunohistological analysis is needed to clarify this point. In the CNS, GLUT3 is found solely in neurons, where its high glucose affinity is relevant for the transport of glucose from the surrounding fluid (Castro et al. 2007; Simpson et al. 2008). Our data suggest that SCs, expressing GLUT3 and GLUT1 in their soma and GLUT3 in the microvilli, could play an important role in glucose distribution in the OE, regulating glucose concentration in the environment surrounding ORNs cilia.

Currently, there is no evidence about the presence of glucose in the ciliary mucus. Nonetheless, it has been reported that glucose is a major component of other epithelial fluids, such us the oviductal fluid, where it is present at millimolar concentrations (Gardner and Leese 1990; Tadokoro et al. 1995; Hugentobler et al. 2008). Moreover, odor transduction occurs in the olfactory cilia, where activation of odorant

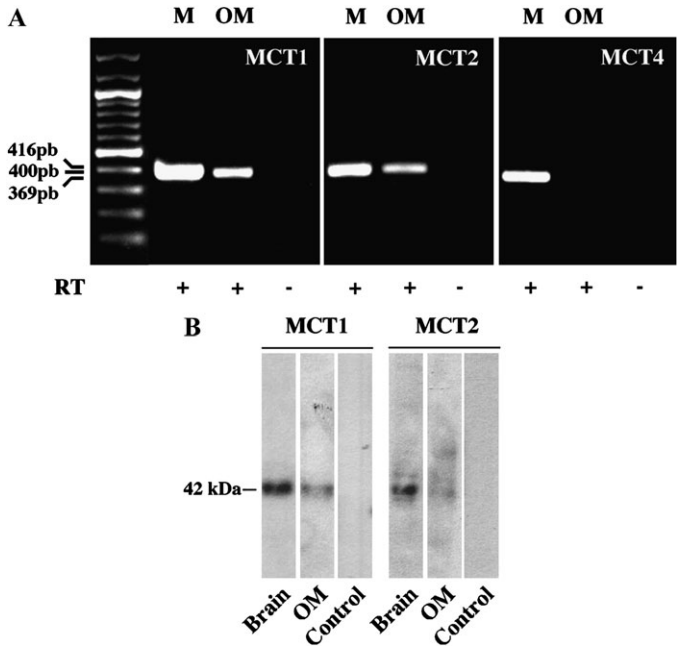

Figure 3 mRNA and protein analysis for MCT expression in the OM. **(A)** Positive labeling for MCT1 and MCT2 mRNAs. M: muscle; (–): negative control. **(B)** MCT1 and MCT2 proteins are expressed in OM. Total brain extract was used as positive control, and preabsorbed antibodies were used as a nonspecific primary antibody–binding control.

receptors leads to an increase in the intracellular Ca^{2+} concentration (for review, see Mombaerts 2004). Olfactory cilia contain a Na^+/K^+-ATPase (Menco et al. 1998) and a plasma membrane Ca^{2+}-ATPasa (PMCA; Weeraratne et al. 2006; Castillo et al. 2007; Antolin et al. 2009). In the absence of Ca^{2+} reservoirs that could capture this divalent cation, this latter enzyme is required, in addition to an Na^+/Ca^{2+} exchanger (Reisert and Matthews 1998), to reestablish the resting Ca^{2+} concentration within the cilia to terminate the odor response. In conditions that cilia do not contain mitochondria, whether glucose plays a role in cilia energy metabolism is not precisely known. However, the findings that glycolytic enzymes are present in cilia (Mayer et al. 2008, 2009) strongly suggest so. GLUT1 and 3 distribution found in the present study suggest that SCs play a role in glucose distribution in the OE and also that ORNs could capture this molecule from the surrounding environment.

GLUT3 was also strongly expressed in the Bowman's glands in the lamina propria, where it can by means of its low K_m, rapidly uptake glucose that diffuses from the blood vessels.

This putative metabolic role of GLUT1 in SCs seems to be well integrated with the expression of MCT1 (a medium affinity lactate transporter, K_m = 4 mM; Simpson et al. 2007), generally present in SCs and strongly expressed close

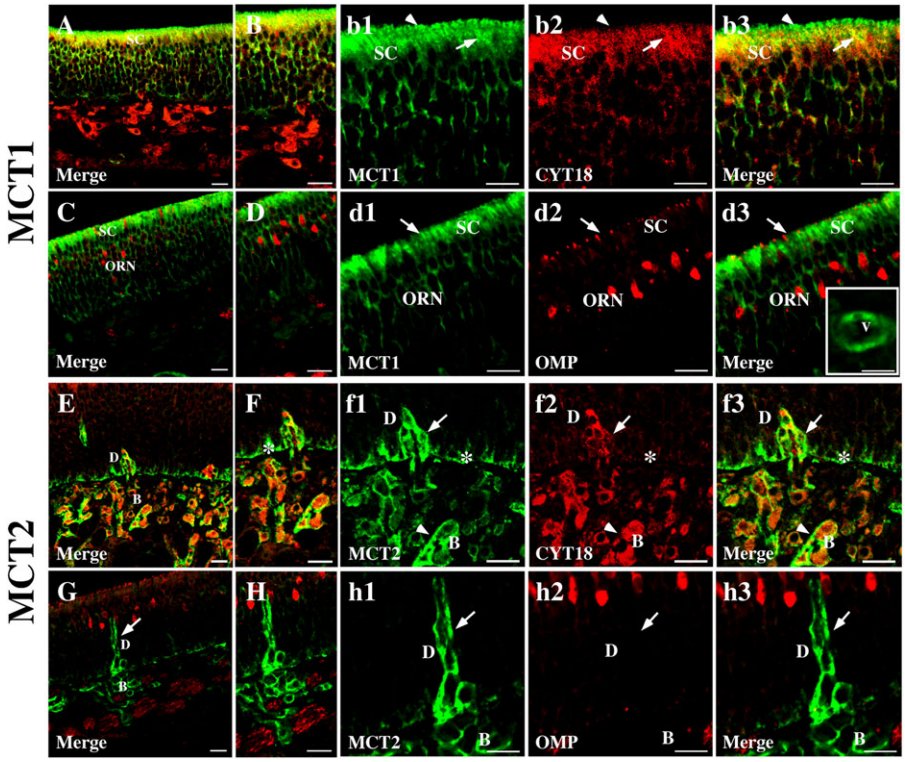

Figure 4 Cellular distribution of MCT1 (**A–d3**) and MCT2 (**E-h3**) in the OM. MCT1 was expressed throughout the whole OE predominantly in the apical portion of the OE (b1, arrow), where it colocalized with CYT18 (A, B, b3). MCT1 was also present in the upper region of the EO (Figure b1, b3, arrowhead) and in the endothelial cells of the blood vessels (d3 insert). MCT2 immunoreactivity was found in cells of the Bowman's gland duct, in the Bowman's gland (E–h3, arrow), and in the basal layer of the OE (E–f3, asterisk). Scale bar, 100 μm; B, Bowman's gland; D, Bowman's gland duct; V, blood vessel.

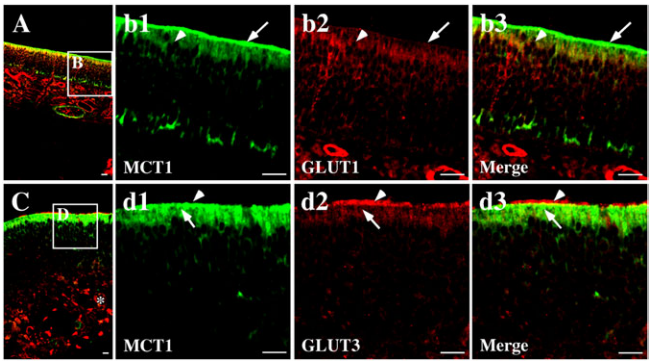

Figure 5 Differential distribution and colocalization of MCT1, GLUT1 (**A–b3**), and GLUT3 (**C–d3**). MCT1 colocalized with GLUT1 in the SC nuclear layer (b3, arrowhead) but not in the outmost part of the OE (b1–b3, arrow). MCT1 overlapped with the GLUT3 signal in the apical portion of the OE (C, d3, arrow) and not in the ciliary/microvillar layer, where only GLUT3 was observed (d3, white arrowhead). GLUT3 was also present in the cells of the Bowman's gland (C, asterisk). Scale bar, 100 μm.

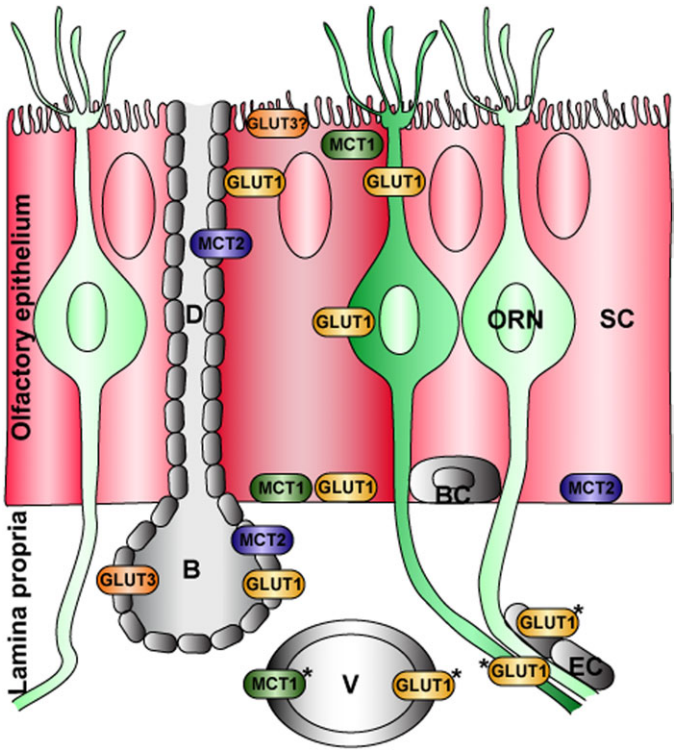

Figure 6 Diagram of the OM depicting the cellular distribution of the glucose and MCTs. Transporters in the endothelial cells of the capillaries and enshething cells were identified based on the morphology of the cells stained and their localization in the lamina propria, *. B, Bowman's gland; BC, basal cell; D, cells of the Bowman's gland duct; EC, ensheathing cell; V, blood vessel.

to the microvilli and basal processes. Thus, SCs may have a role on capturing glucose from the interstitial region and metabolizing it to lactate, which would be subsequently exported by a lactate/H^+ co-transporter to the external environment. Moreover, for the first time, we found evidence that suggest that the Bowman's gland could have an important function in OM lactate metabolism. In these cells, a strong expression of MCT2 was found, where Bowman's gland duct cells could take up lactate for duct cell metabolism. In addition, we found abundant MCT2 labeling in the basal region of the OE, suggesting its presence in SCs processes.

Hence, some similarities of the putative functional interactions between OE cell components and with those between astrocytes and neurons in the CNS are suggested by our results, regarding metabolite transport and possible metabolic interrelationships.

Following the available evidence, we propose the model illustrated in Figure 6. In our model, glucose from the blood is incorporated into the SCs, where it is metabolized to lactate or released into the intercellular and mucous environment. Lactate may be released to the extracellular compartment via MCT1 and incorporated by Bowman's gland duct cells via MCT2. Once in these cells, it could be processed by oxidative metabolism. Cells of the Bowman's duct and gland and SC processes could also incorporate, via MCT2, lactate that was transported from the blood by MCT1 of the endothelial cells.

Funding

This work was supported by MIDEPLAN [ICM-P05-001], FONDECYT [1100682, 1100705, and 1100396], Ring ACT02 and DI-VRIEA-PUCV (Grant Semilla).

References

Antolin S, Reisert J, Matthews HR. 2009. Olfactory response termination involves Ca2+-ATPase in vertebrate olfactory receptor neuron cilia. J Gen Physiol. 135:367–378.

Asan E, Drenckhahn D. 2005. Immunocytochemical characterization of two types of microvillar cells in rodent olfactory epithelium. Histochem Cell Biol. 123:157–168.

Bonen A, Heynen M, Hatta H. 2006. Distribution of monocarboxylate transporters MCT1-MCT8 in rat tissues and human skeletal muscle. Appl Physiol Nutr Metab. 31:31–39.

Castillo K, Delgado R, Bacigalupo J. 2007. Plasma membrane Ca(2+)-ATPase in the cilia of olfactory receptor neurons: possible role in Ca(2+) clearance. Eur J Neurosci. 26:2524–2531.

Castro MA, Pozo M, Cortes C, Garcia Mde L, Concha II, Nualart F. 2007. Intracellular ascorbic acid inhibits transport of glucose by neurons, but not by astrocytes. J Neurochem. 102:773–782.

Chiry O, Pellerin L, Monnet-Tschudi F, Fishbein WN, Merezhinskaya N, Magistretti PJ, Clarke S. 2006. Expression of the monocarboxylate transporter MCT1 in the adult human brain cortex. Brain Res. 1070:65–70.

Cortes-Campos C, Elizondo R, Llanos P, Uranga RM, Nualart F, Garcia MA. 2011. MCT expression and lactate influx/efflux in tanycytes involved in glia-neuron metabolic interaction. PLoS One. 6:e16411.

Eisenberg ML, Maker AV, Slezak LA, Nathan JD, Sritharan KC, Jena BP, Geibel JP, Andersen DK. 2005. Insulin receptor (IR) and glucose

transporter 2 (GLUT2) proteins form a complex on the rat hepatocyte membrane. Cell Physiol Biochem. 15:51–58.

Farbman A. 1992. Cell biology of olfaction. New York, NY: Cambridge University Press.

Garcia CK, Brown MS, Pathak RK, Goldstein JL. 1995. cDNA cloning of MCT2, a second monocarboxylate transporter expressed in different cells than MCT1. J Biol Chem. 270:1843–1849.

Garcia MA, Carrasco M, Godoy A, Reinicke K, Montecinos VP, Aguayo LG, Tapia JC, Vera JC, Nualart F. 2001. Elevated expression of glucose transporter-1 in hypothalamic ependymal cells not involved in the formation of the brain-cerebrospinal fluid barrier. J Cell Biochem. 80:491–503.

Garcia MA, Millan C, Balmaceda-Aguilera C, Castro T, Pastor P, Montecinos H, Reinicke K, Zuniga F, Vera JC, Onate SA, et al. 2003. Hypothalamic ependymal-glial cells express the glucose transporter GLUT2, a protein involved in glucose sensing. J Neurochem. 86:709–724.

Gardner DK, Leese HJ. 1990. Concentrations of nutrients in mouse oviduct fluid and their effects on embryo development and metabolism in vitro. J Reprod Fertil. 88:361–368.

Gerhart DZ, LeVasseur RJ, Broderius MA, Drewes LR. 1989. Glucose transporter localization in brain using light and electron immunocytochemistry. J Neurosci Res. 22:464–472.

Hugentobler SA, Humpherson PG, Leese HJ, Sreenan JM, Morris DG. 2008. Energy substrates in bovine oviduct and uterine fluid and blood plasma during the oestrous cycle. Mol Reprod Dev. 75:496–503.

Hussar P, Tserentsoodol N, Koyama H, Yokoo-Sugawara M, Matsuzaki T, Takami S, Takata K. 2002. The glucose transporter GLUT1 and the tight junction protein occludin in nasal olfactory mucosa. Chem Senses. 27:7–11.

Kream RM, Margolis FL. 1984. Olfactory marker protein: turnover and transport in normal and regenerating neurons. J Neurosci. 4:868–879.

Kumagai AK, Dwyer KJ, Pardridge WM. 1994. Differential glycosylation of the GLUT1 glucose transporter in brain capillaries and choroid plexus. Biochim Biophys Acta. 1193:24–30.

Lachaal M, Rampal AL, Ryu J, Lee W, Hah J, Jung CY. 2000. Characterization and partial purification of liver glucose transporter GLUT2. Biochim Biophys Acta. 1466:379–389.

Maher F, Vannucci SJ, Simpson IA. 1994. Glucose transporter proteins in brain. FASEB J. 8:1003–1011.

Manders EM, Stap J, Brakenhoff GJ, van Driel R, Aten JA. 1992. Dynamics of three-dimensional replication patterns during the S-phase, analysed by double labelling of DNA and confocal microscopy. J Cell Sci. 103(Pt 3): 857–862.

Mayer U, Kuller A, Daiber PC, Neudorf I, Warnken U, Schnolzer M, Frings S, Mohrlen F. 2009. The proteome of rat olfactory sensory cilia. Proteomics. 9:322–334.

Mayer U, Ungerer N, Klimmeck D, Warnken U, Schnolzer M, Frings S, Mohrlen F. 2008. Proteomic analysis of a membrane preparation from rat olfactory sensory cilia. Chem Senses. 33:145–162.

Menco BP, Birrell GB, Fuller CM, Ezeh PI, Keeton DA, Benos DJ. 1998. Ultrastructural localization of amiloride-sensitive sodium channels and Na+, K(+)-ATPase in the rat's olfactory epithelial surface. Chem Senses. 23:137–149.

Millan C, Martinez F, Cortes-Campos C, Lizama I, Yanez MJ, Llanos P, Reinicke K, Rodriguez F, Peruzzo B, Nualart F, et al. 2010. Glial glucokinase expression in adult and post-natal development of the hypothalamic region. ASN Neuro. 2:e00035.

Mombaerts P. 2004. Genes and ligands for odorant, vomeronasal and taste receptors. Nat Rev Neurosci. 5:263–278.

Morris ME, Felmlee MA. 2008. Overview of the proton-coupled MCT (SLC16A) family of transporters: characterization, function and role in the transport of the drug of abuse gamma-hydroxybutyric acid. AAPS J. 10:311–321.

Nakashima T, Kimmelman CP, Snow JB Jr. 1985. Immunohistopathology of human olfactory epithelium, nerve and bulb. Laryngoscope. 95:391–396.

Nomura T, Takahashi S, Ushiki T. 2004. Cytoarchitecture of the normal rat olfactory epithelium: light and scanning electron microscopic studies. Arch Histol Cytol. 67:159–170.

Nualart F, Godoy A, Reinicke K. 1999. Expression of the hexose transporters GLUT1 and GLUT2 during the early development of the human brain. Brain Res. 824:97–104.

Pellerin L, Bergersen LH, Halestrap AP, Pierre K. 2005. Cellular and subcellular distribution of monocarboxylate transporters in cultured brain cells and in the adult brain. J Neurosci Res. 79:55–64.

Pellerin L, Bouzier-Sore AK, Aubert A, Serres S, Merle M, Costalat R, Magistretti PJ. 2007. Activity-dependent regulation of energy metabolism by astrocytes: an update. Glia. 55:1251–1262.

Pellerin L, Magistretti PJ. 1994. Glutamate uptake into astrocytes stimulates aerobic glycolysis: a mechanism coupling neuronal activity to glucose utilization. Proc Natl Acad Sci U S A. 91:10625–10629.

Pierre K, Magistretti PJ, Pellerin L. 2002. MCT2 is a major neuronal monocarboxylate transporter in the adult mouse brain. J Cereb Blood Flow Metab. 22:586–595.

Rand EB, Depaoli AM, Davidson NO, Bell GI, Burant CF. 1993. Sequence, tissue distribution, and functional characterization of the rat fructose transporter GLUT5. Am J Physiol. 264:G1169–G1176.

Reisert J, Matthews HR. 1998. Na+-dependent Ca2+ extrusion governs response recovery in frog olfactory receptor cells. J Gen Physiol. 112:529–535.

Shin BC, McKnight RA, Devaskar SU. 2004. Glucose transporter GLUT8 translocation in neurons is not insulin responsive. J Neurosci Res. 75: 835–844.

Simpson IA, Carruthers A, Vannucci SJ. 2007. Supply and demand in cerebral energy metabolism: the role of nutrient transporters. J Cereb Blood Flow Metab. 27:1766–1791.

Simpson IA, Dwyer D, Malide D, Moley KH, Travis A, Vannucci SJ. 2008. The facilitative glucose transporter GLUT3: 20 years of distinction. Am J Physiol Endocrinol Metab. 295:E242–E253.

Steinke A, Meier-Stiegen S, Drenckhahn D, Asan E. 2008. Molecular composition of tight and adherens junctions in the rat olfactory epithelium and fila. Histochem Cell Biol. 130:339–361.

Tadokoro C, Yoshimoto Y, Sakata M, Imai T, Yamaguchi M, Kurachi H, Oka Y, Maeda T, Miyake A. 1995. Expression and localization of glucose transporter 1 (GLUT1) in the rat oviduct: a possible supplier of glucose to embryo during early embryonic development. Biochem Biophys Res Commun. 214:1211–1218.

Takata K, Hirano H, Kasahara M. 1997. Transport of glucose across the blood-tissue barriers. Int Rev Cytol. 172:1–53.

Tang J, Tang J, Ling EA, Wu Y, Liang F. 2009. Juxtanodin in the rat olfactory epithelium: specific expression in sustentacular cells and preferential subcellular positioning at the apical junctional belt. Neuroscience. 161:249–258.

Vannucci SJ. 1994. Developmental expression of GLUT1 and GLUT3 glucose transporters in rat brain. J Neurochem. 62:240–246.

Weeraratne SD, Valentine M, Cusick M, Delay R, Van Houten JL. 2006. Plasma membrane calcium pumps in mouse olfactory sensory neurons. Chem Senses. 31:725–730.

Weiler E, Benali A. 2005. Olfactory epithelia differentially express neuronal markers. J Neurocytol. 34:217–240.

Wood JP, Chidlow G, Graham M, Osborne NN. 2005. Energy substrate requirements for survival of rat retinal cells in culture: the importance of glucose and monocarboxylates. J Neurochem. 93:686–697.

Yu S, Ding WG. 1998. The 45 kDa form of glucose transporter 1 (GLUT1) is localized in oligodendrocyte and astrocyte but not in microglia in the rat brain. Brain Res. 797:65–72.

Zhao FQ, Keating AF. 2007. Functional properties and genomics of glucose transporters. Curr Genomics. 8:113–128.